Analytical Characterization of Microlithographically Fabricated Iridium-Based Ultramicroelectrode Arrays

Rosemary Feeney, Janet Herdan, Melissa A. Nolan, Sandie H. Tan, Vladislav V. Tarasov, and *Samuel P. Kounaves**

Department of Chemistry, Tufts University, Medford, MA 02155, USA

Received: September 25, 1997
Final version: October 31, 1997

Abstract
The analytical performance of several mercury-coated iridium ultramicroelectrode arrays (IrUMEAs) was studied using square wave anodic stripping voltammetry (SWASV) for determination of cadmium in a pH 4.5 acetate buffer. The microlithographically fabricated IrUMEAs consisted of either 20 or 25 individual disk shaped UMEs, each 10 μm in diameter. The insulating layer utilized in the fabrication process was either silicon dioxide (5000 Å) or silicon nitride (1500 Å or 2500 Å). Calibration plots demonstrated good linearity for cadmium from 0–100 ppb. Standard deviations, detection limits, and correlation coefficients were calculated to determine the stability and reproducibility of the IrUMEAs. Repetitive cycles of depositing and stripping Hg at the IrUMEA surface resulted in increased distortion and loss of the SWASV signal. Atomic force microscopy revealed a subtle transformation in the IrUMEA surfaces.

Keywords: Mercury-coated iridium ultramicroelectrode arrays, Stripping voltammetry, Microlithography

1. Introduction

Voltammetric stripping techniques can offer rapid, low-cost analysis of heavy metals in aqueous systems with sensitivity in the low parts-per-billion range [1]. The use of these techniques has been further stimulated by the advent of ultramicroelectrodes (UMEs), electrodes of micron dimensions. Advantages of UMEs include steady state currents, higher sensitivity due to increased mass transport, and the ability to perform electroanalysis in solutions with high resistance [2]. Thus, UMEs are well suited for in situ analysis of a broad range of natural water systems where very little or no electrolyte is present. However, electronics and the picoampere levels of current hamper the effective use of a single UME. To overcome this limitation, arrays of UMEs (i.e., UMEAs) have been designed to multiply the current signal without losing UME behavior. UMEAs have been used as sensors for various applications such as flow injection analysis [3–5], in cardiovascular monitoring [6] and analyzing organic compounds [7–9]. Using microlithographic technology, UMEAs can be reproducibly fabricated with well-defined geometries. They allow for the versatility of different types of materials and configurations, and also the integration of other chip-based microelectronic devices. They have been fabricated on silicon wafers using a variety of UME substrate materials such as platinum, gold [10] and glassy carbon [5]. Recently, microlithographically fabricated iridium-based UMEAs (IrUMEAs) have been fabricated and demonstrated to be especially advantageous for use with mercury plated films in performing anodic stripping voltammetry (ASV) [11–13]. Iridium has been demonstrated to be a good electrode substrate for mercury films because of its low solubility in mercury (below 10^{-6} wt. %) [14] compared to platinum or gold, and the ability to form a stable mercury hemisphere on its surface [15–19].

Previous articles [11–13] have shown the feasibility of Hg-coated iridium arrays for trace metal determinations. This article describes a study aimed at characterizing the analytical performance of IrUMEAs plated with a semispherical mercury film. The arrays were fabricated by electron beam lithography with different configurations and types of insulating films. These new designs of the IrUMEAs warrant further optimization using electroanalytical methods and surface analysis. The effects of repetitive use of the Hg-coated IrUMEAs on the morphology of the iridium surface were investigated using atomic force microscopy (AFM). The analytical reproducibility and stability of the IrUMEAs were examined using SWASV with Cd^{2+} concentrations in the low ppb range.

2. Experimental

2.1. Electrochemical Apparatus

Chronoamperometry, cyclic voltammetry, linear sweep voltammetry and SWASV experiments were performed with an EG&G PAR Model 263 potentiostat/galvanostat (EG&G PAR, Princeton, NJ) interfaced to a DEC p420-SX microcomputer and using the Model 270 software (EG&G PAR). All voltammetric experiments were performed in a three electrode cell: an IrUMEA, a Ag/AgCl (saturated)//(3 M NaCl) reference electrode (BAS, W. Lafayette, IN) and a Pt wire counter electrode. All potentials were reported relative to the Ag/AgCl (saturated)//(3 M NaCl) reference electrode. Optical observations of the IrUMEAs were made with a Metaval-H (Jena) inverted polarizing microscope equipped with a video imaging system. Surface morphologies were recorded and evaluated using a Nanoscope-E atomic force microscope (Digital Instruments, Santa Barbara, CA).

2.2. Microlithographic Fabrication of Iridium Arrays

The IrUMEAs were fabricated on a standard 4-inch silicon wafer substrate. The wafer was cleaned and a 5000 Å layer of silicon dioxide was grown on the surface. After coating with photoresist and patterning, a 300 Å titanium layer and a 1000 Å iridium layer were deposited on the surface by electron beam evaporation. A layer of aluminum was deposited as an interconnect trace between the IrUMEAs and the bond pads. A lift-off process was used to leave the desired iridium pattern. The conductors were protected and insulated by a layer of either silicon nitride (1500 Å or 2500 Å) or silicon dioxide (5000 Å) deposited by low-temperature plasma enhanced chemical vapor deposition (PECVD). The insulating layer was patterned and selectively plasma etched to expose the active iridium surfaces.

Two different UMEA patterns were used, one consisted of a ‘square’ UMEA that contained 25 individual 10 μm iridium disks (Fig. 1A) and the second was a concentric ‘circular’ UMEA that

  1040-0397/98/0202-0089 $ 17.50+.50/0

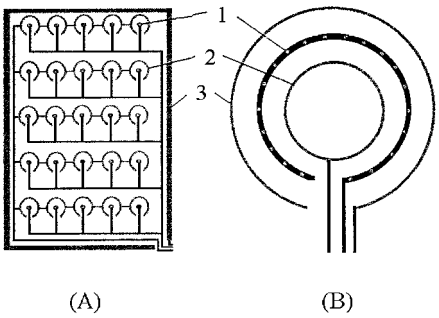

Fig. 1. A) The square array design consists of 25 disk iridium UMEs (1). Each UME is surrounded by a ring element (2) which can be utilized as a reference electrode. The 25 disk UMEs and the reference electrodes are surrounded by a square element (3) which can be used as the counter electrode. B) The circular design consists of three concentric rings. The middle ring contains 20 disk UMEs (1). The other two rings can be used as an on-chip reference (2) and counter (3) electrode.

contained 20 individual 10 μm iridium disks (Fig. 1B). Each chip consists of two UMEAs that can be addressed individually. The chips were diced (5 mm $\times$ 16 mm) and glued to a custom-designed printed circuit (PC) board (CFC, Waltham, MA) with epoxy (Epo-Tek 905, Epoxy Technology Inc., Billerica, MA). The bonding pad on the chip was connected to the PC board using a West Bond wire bonder with 1.25 micron Au wire (99.99 %, Williams Advanced Materials, Buffalo, NY). The gold wire was protected by a glob type epoxy (87-GT, Epoxy Technology Inc., Billerica, MA), that was cured at 70 °C for three hours.

2.3. Deposition and Stripping of the Mercury

The IrUMEA was conditioned by hydrogen evolution in 0.1 M $HClO_4$ by holding the potential at -1.9 V for 120 s. Mercury was deposited from a 8×10^{-3} M Hg^{II} in 0.1 M $HClO_4$ solution at a potential of -0.4 V for 600 s. Deposition of mercury on all the individual IrUMEs was confirmed optically. After the experiments were performed, the mercury was stripped by linear sweep voltammetry going from -0.3 V to 0.3 V at a scan rate of 20 mV/s in 1 M KSCN. The condition of the individual IrUMEs was optically ascertained after the mercury stripping step. The arrays were stored dry in a polyethylene container when not in use.

2.4. Determination of Cadmium

Five standard additions of 20 ppb cadmium were determined in a 0.02 M acetate buffer (pH 4.5). Cadmium was deposited into the mercury by holding the potential at -0.9 V for 240 s. The Cd was stripped by scanning the potential anodically using SWASV with a pulse height of 25 mV, frequency of 60 Hz, conditioning potential of -0.3 V and conditioning time of 200 s.

2.5. Reproducibility and Surface Effects

Two different approaches were used to investigate the reproducibility and surface morphology effects of six different arrays (circular and square designs) consisting of silicon dioxide (5000 Å) and silicon nitride (1500 Å and 2500 Å) insulation layers. In both cases the arrays were evaluated using a 60 ppb cadmium solution and the same parameters as above. As part of the 'same Hg coating' study, one mercury coating was used to perform ten consecutive measurements of cadmium. The mercury coating was electrochemically stripped as described above and the surface was evaluated using an optical microscope. The 'new Hg coating' study involved stripping and replating mercury after each cadmium determination. The optical microscope was used to observe the condition of the iridium surface each time the mercury was stripped.

2.6. Reagents

All solutions were prepared with 18 MΩ cm deionized water from a Barnstead Nanopure system (Barnstead Co., Dubuque, IA). All glassware was stored in 8 M HNO_3 for a week and rinsed thoroughly with 18 MΩ cm deionized water. The acetate buffer solutions were prepared with 99.99+ % sodium acetate (Fluka) and glacial acetic acid (Fisher Scientific). Metal solutions were prepared from 99.999+ % Cd $(NO_3)_2$ (Aldrich) and $Hg(NO_3)_2$ (Johnson Matthey). All other solutions were prepared with ACS grade reagents.

3. Results and Discussion

In this study the analytical performance of the arrays was examined. The overall success rate of the fabrication process in this study was approximately 90 %. This high rate of success was one of the major advantages of microlithography due to the uniformity of the deposition process across the wafer. The 10 % failure rate could be attributed to the multiple steps in preparing the IrUMEA/PC board electrochemical system, such as general handling, wiring bonding, and application of the epoxy.

To verify that these arrays act as UMEs, a cyclic voltammogram for $K_3Fe(CN)_6$ was obtained. A classical sigmoidal response (Fig. 2) was obtained for both configurations of UMEAs, indicating that a diffusion controlled process and a steady-state current were achieved. This also indicated that a separation distance of at least 100 μm between individual UME disks is more than sufficient to allow for the individual diffusion spheres for each UME. Thus, by using such arrays one can obtain an increased signal while maintaining theoretical ultramicroelectrode behavior.

The analytical performance was established by obtaining three calibration plots for each type of array. Figure 3A shows a typical series of SW stripping voltammograms for five standard additions of Cd^{2+} to a 0.02 M acetate buffer solution (pH 4.5), while Figure 3B shows the typical SWASV reverse (a), forward (b), and net (c) current response. The linear regression coefficients for the results using the square, circular, silicon nitride, and silicon dioxide UMEAs are shown in Table 1. The silicon dioxide insulated array exhibited the best linearity for both designs. The *y*-intercepts for most UMEAs were slightly below zero, probably as a result of shifts in the individual baselines. A noticeable trend in the data for all but

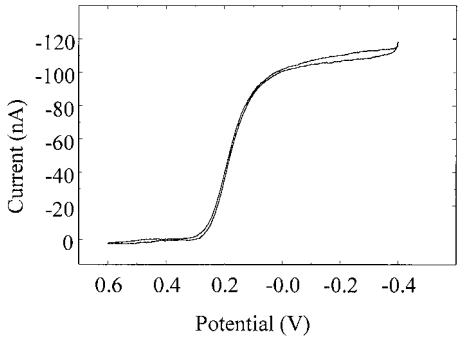

Fig. 2. Cyclic voltammogram of 6 mM ferricyanide in 0.1 M HNO_3 was obtained with circular designed, silicon dioxide coated IrUMEA. The scan rate was 10 mV/s.

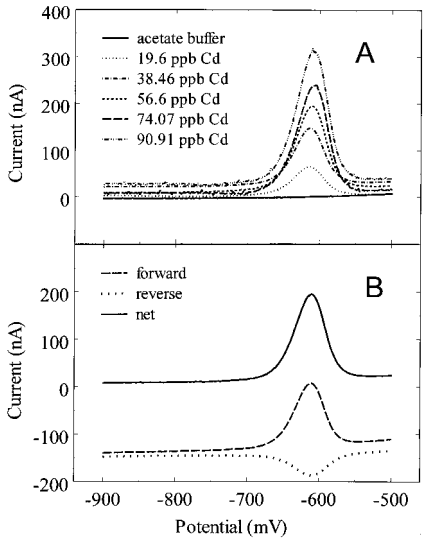

Fig. 3. A) The SWASV for standard additions of 20 ppb cadmium to a 0.02 M acetate buffer (pH 4.5) for a silicon nitride (1500 Å) IrUMEA. Conditions: SW pulse amplitude: 25 mV; frequency: 60 Hz; deposition time: 240 s; deposition potential: −0.9 V; conditioning potential: −0.3 V; conditioning time: 200 s. B) Typical forward (a), reverse (b), and net (c) currents for an IrUMEA in a solution containing 60 ppb Cd, showing classical reversible behavior at a mercury coated UMEA.

the 1500 Å silicon nitride coated UMEAs was the resulting decreased sensitivity in going from the first to the third run. This is presumed to be an indication of either increased fouling of the UME surfaces or changes in the surface morphology of the iridium or the insulating layer. However, even for the third and least sensitive run, measurable current signals were obtained for 20 ppb cadmium with detection limits estimated at 3.58 and 5.96 ppb for the silicon nitride (2500 Å, 1500 Å) UMEAs, and 3.84 ppb for the silicon dioxide (5000 Å) UMEA. An increased sensitivity was found when thicker insulating layers were utilized, as indicated by the calibration slopes in Table 1. The use of either silicon nitride or silicon dioxide layers did not dramatically affect the sensitivity of the UMEAs, as long as the insulating thickness was at least 2500 Å.

Two different approaches were used for investigating the reproducibility and surface morphology effects with the six different IrUMEAs. First, the peak stripping current was measured for ten consecutive runs using the same mercury coating per array. The results for each type of UMEA (Fig. 4) were reported in Table 2 with the average and standard deviation values. The current at each individual UME in the array contributed to the total current observed and thus all of the square UMEAs were expected to yielded approx. a 25 % higher peak current signal than the circular ones. However, the peak currents for all the runs of the 5000 Å square UMEA and the first five runs of the 2500 Å square UMEA were about 2–3 times higher than expected for the equivalent circular type. In terms of reliable response though, all except the 2500 Å gave reproducible linear relationships between current and concentration for all ten runs using the same mercury coating for the determination of ppb level of the metal. In general, the overall responses of the IrUMEAs were stable for ten consecutive runs using the same mercury coating. The 2500 Å silicon nitride UMEA demonstrated a slight instability after the fifth run. This was not a typical response and may be the result of the loss of mercury during the experiment, but a plausible explanation for the decrease in current response could not be determined.

In the second approach, a new mercury coating was deposited before each measurement of the 60 ppb cadmium solution. The renewed mercury coating allowed us to check for any possible fouling of the mercury during the calibration plot experiments that might lead to decreased sensitivity. Even though the fresh mercury coatings would be expected to provide more reproducible results, they did not as indicated by the larger standard deviation values in Table 2. The fluctuations in each peak height (not shown) were noticeably greater than those obtained with the same mercury coating for all the other types of UMEA. Thus, it appeared that fouling of the mercury was not linked to the erratic performance of the IrUMEAs. Unlike the first approach, the square design did not give higher current signals. Even though there were more UMEs in the square design, there was also a greater probability for failure because there were 25 areas where the iridium UME pad overlapped

Table 1. Effects of UMEA configuration and insulation on calibration plot for the IrUMEAs in a 60 ppb Cd solution.

Array	*Regression coefficient Mean ± std. dev.*	*Y-intercept Mean [nA]*	*Calibration slope*	
			1st Run	*3rd Run*
silicon nitride 2500Å, square	0.977 ± 0.024	−5.861	4.247	1.315
silicon nitride 2500Å, circle	0.980 ± 0.015	−7.466	3.045	0.6835
silicon dioxide 5000Å, square	0.991 ± 0.013	−5.815	5.178	3.203
silicon dioxide 5000Å, circle	0.989 ± 0.009	0.6430	3.727	0.4788
silicon nitride 1500Å, square	0.982 ± 0.022	3.675	2.060	2.002
silicon nitride 1500Å, circle	0.981 ± 0.018	−1.365	1.352	3.081

Table 2. Current responses for the IrUMEAs in a 60 ppb Cd solution. Column 1: the average of 10 consecutive measurements with the same mercury coating. Column 2: average measurements in the same cadmium solution, but each run with a new mercury coating.

Array	*UMEA with same Hg coating Mean ± std. dev. [nA]*	*UMEA with new Hg coating Mean ± std. dev. [nA]*
silicon dioxide 5000 Å, circle	114 ± 9.2	244.8 ± 13.2
silicon nitride 1500 Å, circle	124.1 ± 11.4	251.6 ± 18.3
silicon nitride 2500 Å, circle	53.93 ± 9.99	90.24 ± 21.9
silicon dioxide 5000 Å, square	305.5 ± 13.1	149.3 ± 88.5
silicon nitride 1500 Å, square	140.4 ± 13.4	108.5 ± 56.8
silicon nitride 2500 Å, square	223.6 ± 47.0	134.6 ± 52.9

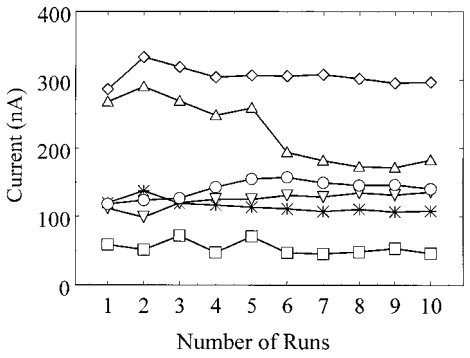

Fig. 4. The stripping peak-current response of ten consecutive runs for a 60 ppb cadmium solution using the same mercury coating for each of six different UMEAs. (*) 5000 Å silicon dioxide, circular; (◇) 5000 Å silicon dioxide, square; (□) 2500 Å silicon nitride, circular; (Δ) 2500 Å silicon nitride, square; (∇) 1500 Å silicon nitride, circular; (○) 1500 Å silicon nitride, square.

with the aluminum interconnect trace. This may have created multiple stress points compared to the circular design which only has one connection to the aluminum interconnect.

It was determined that the morphology of the iridium surface was directly related to the abnormal variations in peak height. Optical microscopy revealed that after the removal of the mercury coating, the iridium surfaces had become fouled with small micron-size accumulations, independent of the insulator type and the design. This prevented formation of a uniform coating of mercury for the subsequent analysis and was probably the cause for the decrease in sensitivity that was evident during the three calibration runs for each array.

AFM images of the surface of IrUMEAs, before and after use, are shown in Figures 5A–C. The iridium surface of all the UMEs, before use, were relatively smooth with no apparent accumulations or irregularities (Fig. 5A). After the three calibration runs, the circular UMEA with the 1500 Å silicon nitride coating showed good linearity and sensitivity for all runs. In addition, AFM images (Fig. 5B) showed a surface that was relatively uneffected by the experimental conditions, with only a few submicron features visible. In contrast, on the circular 2500 Å silicon nitride array not only can one see, both visually and via AFM, some substantial micron sized accumulations (Fig. 5C), but they coincided with decreasing electroanalytical sensitivity. The AFM image showed a large number of deposits on the Ir surfaces, which was consistent for the other UMEs. The accumulations appeared to be pyramidal in shape with an approximate height of 2 microns. Most accumulations were found clustered together, although some were scattered across the 10 μm iridium disks. This evidence supported our supposition that the condition of the iridium surface was directly responsible for the highly variable calibration sensitivities. The contamination of the UME surfaces would appear to interfere with the deposition of a new mercury semisphere and with the analysis performed at an existing one. The identity of this accumulated material has been investigated in detailed [20] and has been found to be mercurous chloride (Hg_2Cl_2).

4. Conclusion

The circular design demonstrated better analytical performance even though there were fewer UMEs. The physical stress at each exposed UME disk was minimized because they were not individually connected as in the square design. The results of the calibration plots confirmed that the UMEAs provide varying

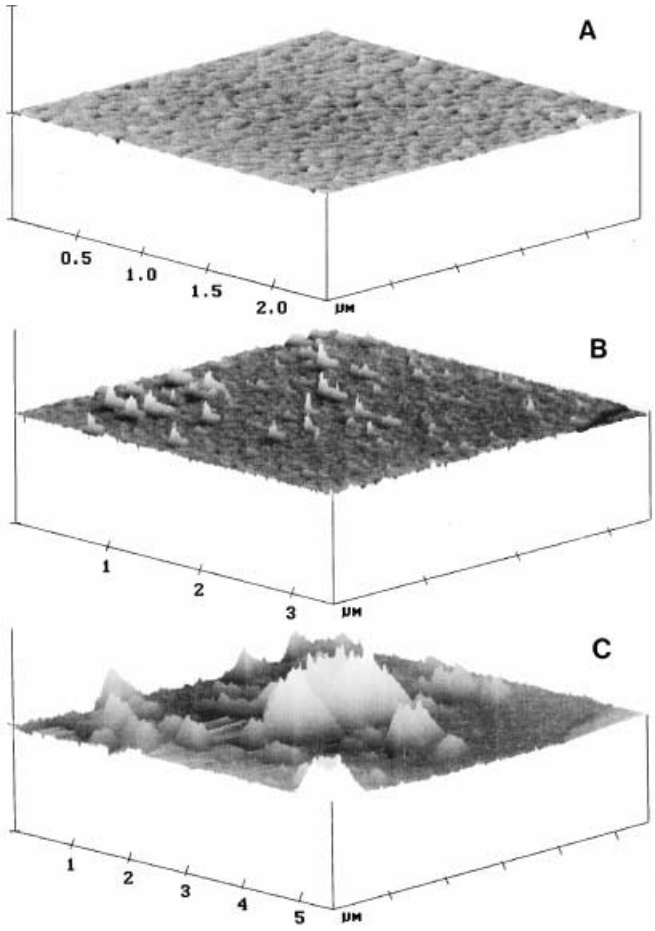

Fig. 5. AFM images of the Ir surface of two IrUMEAs. A) Typical image before use. B) Image of a circular type with 1500 Å silicon nitride insulation after the calibration study. The scan-size and -rate were 3.4 μm and 3.39 Hz, respectively. **C**) Same type as (B) but with 2500 Å silicon nitride, taken after use in the calibration study. The scan-size and -rate were 5.6 μm and 3.39 Hz, respectively.

sensitivities, but they also demonstrated a consistently reproducible relationship between current and concentration. The main reason for the variation in current response of the IrUMEAs was ultimately the fouling of the iridium surfaces. Stripping mercury between runs was not effective in eliminating this phenomenon but led to a higher degree of fouling.

5. Acknowledgements

This work was supported in part by grants from the Environmental Protection Agency through the Northeast Hazardous Substance Research Center at NJIT, and the National Science Foundation (CHE-9256871). We also wish to thank the School of Engineering – Microsystems Technology Laboratories, at the Massachusetts Institute of Technology for providing the microlithographic fabrication of the UMEA chips.

6. References

[1] J. Wang, *Stripping Analysis*, VCH Publishers, Deerfield Beach FL **1985**.
[2] R.M. Wightman, D.O. Wipf, *Electroanalytical Chemistry*, Vol.15 (Ed: A.J. Bard), Marcel Dekker, New York **1989**.

[3] M. Paeschke, F. Dietrich, A. Ulig, R. Hintsche, *Electroanalysis*, **1996**, *8*, 891.
[4] T. Dimitrakopoulos, P.W. Alexander, D.B. Hibbert, *Electroanalysis* **1996**, *8*, 438.
[5] P.R. Felden, T. McCreedy, *Anal. Chim. Acta* **1993,** *273*, 111.
[6] V. Cosofret, M. Erdosy, T.A. Johnson, R.P. Buck, R.B. Ash, M. R. Neuman, *Anal. Chem*. **1995**, *67*, 1647.
[7] Q. Chen, J. Wang, G. Rayson, B. Tian, Y. Lin, *Anal. Chem*. **1993**, *65*, 251.
[8] R. Hintsche, M. Paeschke, U. Wollenberger, U. Schnakenberg, B. Wagner, T. Lisec, *Biosens. Bioelectron.* **1994**, *9*, 697.
[9] G. Sreenivas, S.S. Ang, I. Fritsch, W.D. Brown, G.A. Gerhardt, D.J. Woodward, *Anal. Chem*. **1996**, *68*, 1858.
[10] A. Uhlig, U. Schnakenberg, R. Hintsche, *Electroanalysis* **1997**, *9*, 125.
[11] S.P. Kounaves, W. Deng, P.R. Hallock, G.T.A. Kovacs, C. Storment, *Anal. Chem.* **1994**, *66*, 418.
[12] G.T.A. Kovacs, C.W. Storment, S.P. Kounaves, *Sens. Actuators B* **1995**, *23*, 41.
[13] C. Belmont, M.L. Tercier, J. Buffle, G.C. Fiaccabrino, M. Koudelka-Hep, *Anal. Chim. Acta* **1996**, *329*, 203.
[14] C. Guminski, Z. Galus, in *Solubility Data Series-Metals In Mercury*, (Eds: C. Hirayama, C. Guminski, Z. Galus) Pergamon Press, Oxford **1986**.
[15] S.P. Kounaves, J.J. Buffle, *J. Electroanal. Chem*. **1988**, *239*, 113.
[16] S.P. Kounaves, W. Deng, *Anal. Chem*. **1993**, *65*, 375.
[17] S.P. Kounaves, W. Deng, *J. Electroanal. Chem*. **1991**, *301*, 77.
[18] C. Wechter, J. Osteryoung, *Anal. Chem.* **1989**, *61*, 2092.
[19] J. Wang, B. Tian, M. Jiang, *Anal. Chem.* **1997**, *67*, 1657.
[20] M.A. Nolan, S.P. Kounaves, unpublished.

Equipment News

101 Potentiostat

Cypress Systems has introduced a new low cost potentiostat, designed to give the user all the convenience of microprocessor-based digital interface, with the technical advantage of an analog potentiostat. The OMNI-101 comes with an RS232 interface and Windows software, a computer, and three-electrode kit, and can perform 10 different techniques. Cypress Systems, Lawrence, KS.

Multi-Parameter Meter

The new Orion Model 1260 multi-parameter meter is a compact analyzer, integrating measurements of pH, ion-selective electrodes, dissolved oxygen, , BOD, salinity, conductivity and temperature. It has been designed for the water and wastewater laboratories. Orion Research, Beverly, MA.

Scanning Electrochemical Microscope

The new CH1900 Scanning Electrochemical Microscope consists of a digital function generator, a bipotentiostat, high resolution data acquisition circuitry, a three dimensional micropositioner, an Inchworm motor controller, and sample and cell holder. The three dimensional micropositioner has a spatial resolution better than one nanometer, and it allows a maximum traveling distance of several centimeters. The potential control range of the bipotentiostat is ±3.275V and the current range is ±10mA. The instrument is capable of measuring current down to subpicoamperes. In addition to SECM imaging, two other modes of operation are provided for scanning probe applications: The Probe Scan Curve mode allows the probe to move in X, Y, or Z direction while the probe and substrate potentioals are controlled and current are measured, CH Instruments, Cordova, TN.

Low Noise Carbon Fiber Potentiostat

World Precistion Instruments offers a low-cost, low-noise, compact potentiostat for electrochemical detection of catecholamines and indolamines using carbon fiber microelectrodes. The MicroC instrument offers a built in electrode activation feature, and a battery life of over 1000h. Also available various carbon and metal microelectrodes. World Precision Instruments, Sarasota, FL.

Total System

Arbin Instruments offers a universal multielectrode, mulitstation potentiostat/galvanostat for the simultaneous testing of multiple electrodes. The MSTAT system offers current output down to 200µs and offers current output up to 200A. Arbin Instrument, College Station, TX.

Awards

Professor A. J. Bard of the University of Texas – Austin is the recipient of the US National Academy of Sciences Award in Chemical Sciences. Dr. Bard was selected for his fundamental contributions to mechanistic electrochemistry, electochemiluminescence, and scanning electrochemical microscopy.